



U.S. DEPARTMENT OF
ENERGY

PNNL-18212

Prepared for the U.S. Department of Energy
under Contract DE-AC05-76RL01830

Update of Gap Release Fractions for Non-LOCA Events Utilizing the Revised ANS 5.4 Standard

CE Beyer
PM Clifford

February 2009



Pacific Northwest
NATIONAL LABORATORY

DISCLAIMER

This report was prepared as an account of work sponsored by an agency of the United States Government. Neither the United States Government nor any agency thereof, nor Battelle Memorial Institute, nor any of their employees, makes **any warranty, express or implied, or assumes any legal liability or responsibility for the accuracy, completeness, or usefulness of any information, apparatus, product, or process disclosed, or represents that its use would not infringe privately owned rights.** Reference herein to any specific commercial product, process, or service by trade name, trademark, manufacturer, or otherwise does not necessarily constitute or imply its endorsement, recommendation, or favoring by the United States Government or any agency thereof, or Battelle Memorial Institute. The views and opinions of authors expressed herein do not necessarily state or reflect those of the United States Government or any agency thereof.

PACIFIC NORTHWEST NATIONAL LABORATORY
operated by
BATTELLE
for the
UNITED STATES DEPARTMENT OF ENERGY
under Contract DE-AC05-76RL01830

Update of Gap Release Fractions for Non-LOCA Events Utilizing the Revised ANS 5.4 Standard

CE Beyer
PM Clifford¹

February 2009

Pacific Northwest National Laboratory
Richland, Washington 99352

¹ Paul M. Clifford, U.S. Nuclear Regulatory Commission

Acronyms and Abbreviations

ANS	American Nuclear Society
ANSI	American National Standards Institute
BIGR	Fast-pulse graphite reactor
BWR	boiling-water reactor
cal/gm	calorie/gram
EOL	end of life
FGR	Fission gas release
FRAPCON	fuel rod performance code
GWd/MTU	gigawatt day per metric ton uranium
IFA	instrumented fuel assembly
JAERI	Japan Atomic Energy Research Institute
kW/ft	kilowatt per foot
LHGR	linear heat generation rate
LOCA	loss-of-coolant accident
LWR	light-water reactor
MOX	mixed oxide fuel
ms	millisecond
NCLO	no cladding liftoff
NRC	U.S. Nuclear Regulatory Commission
NSRR	Nuclear Safety Research Reactor
PWR	pressurized-water reactor
R/B	release to birth
RIA	reactivity initiated accident
UTL	upper tolerance level
VVER	Soviet-designed pressurized water reactor

Contents

1.0	Introduction	1
2.0	Gap Release Fractions for Accidents without Large Fuel Temperature Increases	2
2.1	Background of Proposed Revised ANS 5.4 Standard	2
2.1.1	Uncertainties in Revised ANS 5.4 Standard and Comparisons to Release Data	3
2.1.2	Application of Proposed Revised ANS 5.4 Using a Fuel Performance Code	4
2.2	FRAPCON-3.3/ANS 5.4 Calculated Gap Release Fractions	4
2.2.1	PWR Analyses	4
2.2.2	BWR Analyses	5
2.2.3	Assumed Analysis Uncertainties	6
2.2.4	Discussion and Recommendations for Gap Release Fractions	6
3.0	Gap Release Fractions for Reactivity Initiated Accident	8
3.1	Discussion of RIA Release Data and Recommendations for Gap Fractions	8
3.2	Example Determination of Gap Release Fractions for a RIA	11
4.0	Conclusions and Limitations	12
5.0	References	13
	Appendix A : Code Input including Power Histories and Axial Power Shapes Used for FRAPCON-3.3/ANS 5.4 Analyses	21
	Appendix B : Compilation of Fission Gas Release Data from RIA Tests in CABRI, NSRR and BIGR	30

Figures and Tables

Figures

Figure 1. Operating Range of Data Used to Develop and Verify the ANS 5.4 Model	17
Figure 2. Draft ANS 5.4 Standard Model Comparison of Prediction to Measured I-131 Release Data Assuming a Factor of 5 Multiplier on Prediction Results in a 95/95 UTL	18
Figure 3. ANS 5.4 Model Best Estimate Prediction of R/B I-131 Data from Halden Experiments IFA-504 and IFA-558	18
Figure 4. Predicted R/B Release for I-131 as a Function of Burnup Illustrating Peak Release Occurs at the Maximum Burnup at which Maximum Rod Power is Achieved.....	19
Figure 5. Predicted Release Fraction Normalized to Produced Inventory for Kr-85 (Long-Lived) Isotope as a Function of Burnup Illustrating Peak Release Occurs at EOL.....	19
Figure 6. Stable Fission Gas Release Data as a Function of Peak Fuel Enthalpy Increase from Simulated RIA Tests in CABRI, NSRR, and BGR Test Reactors	20
Figure A-1. LHGR Bounding Limit for PWRs Up to 34 GWd/MTU (Peak Nodal Burnup), Beyond this Burnup LHGR Based on Depletion For Current Cores.....	22
Figure A-2. Assumed PWR Power History #1	22
Figure A-3. Assumed PWR Power History #2	23
Figure A-4. Assumed PWR Power History #3	23
Figure A-5. Assumed PWR Power History #4	24
Figure A-6. Assumed PWR Power History #5	24
Figure A-7. PWR Normalized Axial Power Shapes, the BU Label is the Rod Average Burnup (GWd/MTU) Level the Shape Begins	25
Figure A-8. LHGR Bounding Limit for BWRs Up to 70 GWd/MTU (Peak Nodal Burnup).....	26
Figure A-9. Assumed BWR Power History #1	26
Figure A-10. Assumed BWR Power History #2.....	27
Figure A-11. Assumed BWR Power History #3.....	27
Figure A-12. Assumed BWR Power History #4.....	28
Figure A-13. Assumed BWR Power History #5.....	28
Figure A-14. BWR Normalized Axial Power Shapes, the BU Label is the Rod Average Burnup (GWd/MTU) Level at Which the Axial Shape Begins.....	29

Tables

Table 1. PWR Fuel Rod Release Fractions, R/B, for Isotopes with Half-Lives Greater Than 1 Hour for Five Bounding Power Histories up to 68 GWd/MTU Peak Node Burnup and Rod Average 62 GWd/MTU (All Burnups are in GWd/MTU)	15
Table 2. BWR Fuel Rod Release Fractions, R/B, for Isotopes with Half-Lives Greater Than 1 Hour for Five Bounding Power Histories up to 70 GWd/MTU Peak Node Burnup and Rod Average 62 GWd/MTU (Burnups are rod average in GWd/MTU).....	15
Table 3. PWR and BWR Fuel Rod Peak Gap Release Fractions, R/B, Based on Peak Values from Tables 1 and 2 ³	16
Table 4. Local Gap Release Fractions for Reactivity Initiated Accidents	16
Table A-1. FRAPCON-3.3 Input Parameters for PWR and BWR Analyses.....	21

1.0 Introduction

The U.S. Nuclear Regulatory Commission (NRC) has established guidance on fission product release fractions from the fuel cladding gap of fuel rods that have been breached during postulated accidents for use in determining dose consequences from these events. The guidance for fission product gap release fractions for non-loss-of-coolant accident (LOCA) events has been defined in the following regulatory guides:

- Regulatory Guide 1.5, “Assumption Used for Evaluating the Potential Radiological Consequences of a Steam Line Break Accident for Boiling Water Reactors” (Reference 1)
- Regulatory Guide 1.25, “Assumption Used for Evaluating the Potential Radiological Consequences of a Fuel Handling Accident in the Fuel Handling and Storage Facility for Boiling Water and Pressurized Water Reactors” (Reference 2)
- Regulatory Guide 1.77, “Assumption Used for Evaluating the Potential Radiological Consequences of a Control Rod Ejection Accident for Pressurized Water Reactors” (Reference 3)
- Regulatory Guide 1.195, “Methods and Assumptions for Evaluating Radiological Consequences of Design Basis Accidents at Light-Water Nuclear Power Reactors” (Reference 4).

In addition, Regulatory Guide 1.183 (Reference 5) was issued to provide guidance for alternative source terms and acceptable radiological analysis assumptions for both LOCA and non-LOCA events. The objective of the work reported here is to provide a recommended replacement for Section 3.2 of Regulatory Guide 1.183. When approved, the release fractions recommended in this report will supersede those in the above regulatory guides for non-LOCA accidents.

Fission product gap release fractions are different for normal operation where release is only diffusion controlled versus those with sudden large temperature increases, such as for a reactivity initiated accident (RIA) where release is only partially diffusion controlled; therefore, two different approaches are necessary to estimate the gap release fractions. This report will address gap release from two different non-LOCA accidents; 1) those that do not involve large fuel temperature increases such as fuel handling and steam line break accidents, and 2) the RIA that involves a large fuel temperature increase.

Regulatory guides 1.183 and 1.77 recommend a gap release fraction of 0.10 for both noble gases and iodines for a RIA event (boiling-water reactor [BWR] control rod drop or pressurized-water reactor [PWR] control rod ejection). Fuel rod tests have been performed in the CABRI, NSRR, and BGR test reactors to simulate reactivity-initiated transients. Fission gas release data collected from these fuel test rods have demonstrated that the stable gas release can be greater than the 0.10 fraction recommended in the two regulatory guides. As a result, the data from these test reactors will be used to recommend new gap release fractions for RIA events.

A discussion of gap release fractions for accidents without large fuel temperature increases is provided in Section 2; gas release fractions for RIAs are provided in Section 3; and Section 4 provides a summary. The FRAPCON-3.3 fuel rod performance code (Reference 6) input values for calculations in Section 2 are provided in Appendix A and RIA data are provided in Appendix B.

2.0 Gap Release Fractions for Accidents without Large Fuel Temperature Increases

Gap release fractions in accidents that do not involve large fuel temperature increases (such that the gap fractions are due to gas atom diffusion during normal operation) were determined using the proposed revision[†] to the American Nuclear Society (ANS) 5.4 standard (Reference 7) entitled “Method for Calculating the Fractional Release of Volatile Fission Products from Oxide Fuel.” The proposed revision to the ANS 5.4 standard does not cover accidents that achieve high fuel temperatures as experienced during a RIA; therefore, this event needs to be addressed separately.

In Regulatory Guide 1.183, the Table 3 gap fractions were determined from analyses using FRAPCON-3.0 (Reference 8) and the previous 1982 ANS 5.4 standard. The FRAPCON-3 code provides predicted fuel temperatures needed by the ANS 5.4 model to predict gap release fractions. The reason for updating the ANS 5.4 standard and the Table 3 values in Regulatory Guide 1.183 is that the 1982 ANS 5.4 standard significantly over predicts the iodine release fractions. In addition, current operation in plants is at or close to the limit on rod average powers of 6.3 kilowatt per foot (kW/ft) at burnups above 54 gigawatt day per metric ton uranium (GWd/MTU) as recommended for the gap fractions in Regulatory Guide 1.183. It is not possible to eliminate a power and burnup limit on release fractions because fission product release is highly dependent on both of these parameters. Therefore, this proposed revision to Regulatory Guide 1.183 will increase the rod power and burnup envelope from the 6.3 kW/ft (rod average) at 54 GWd/MTU burnup. The revised power envelope in Figures A-1 (for PWRs) and A-8 (for BWRs) provided in Appendix A was created to be equal to or to bound maximum rod powers in current reactor cores. These peak rod power envelopes versus burnup were used to calculate the new release fractions using a fuel performance code and the proposed revised ANS 5.4 standard.[†]

The gap release values calculated in this report involve the use of the updated FRAPCON-3.3 fuel performance code (Reference 6) with the proposed revised ANS 5.4 standard equations implemented in the code to determine the release-to-birth (R/B) fractions of the volatile radioactive isotopes of noble gases (xenon and krypton), iodines, and cesiums. Those radioactive isotopes with half-lives less than 60 days have utilized the release equations recommended by the proposed revised ANS 5.4 standard; this includes all of the noble gases except Kr-85 and the iodines. For those isotopes with very long half-lives, such as Kr-85, Cs-134, and Cs-137 with half-lives of 10.76 years, 2.07 years, and 30.1 years, respectively, the steady-state fission gas release model in the FRAPCON-3.3 code was used as recommended by the proposed revised ANS 5.4 standard. The calculational results include the proposed revised ANS 5.4 recommended uncertainties for those short-lived isotopes (half-lives less than 60 days) and the FRAPCON-3.3 release uncertainties, both at a 95/95 tolerance level.

2.1 Background of Proposed Revised ANS 5.4 Standard

The ANS 5.4 standard has been recently revised (but has not received final approval from American National Standards Institute (ANSI) as of January 2009) based on in-reactor release measurements of radioactive noble gas and iodine isotopes. The previous 1982 standard was based only on the release of stable noble gases with no in-reactor measurements of iodine release. As a result, the previous 1982 standard for iodine release is based on a very small amount of out-of-reactor (heating) release data that provided higher release values than observed from the recent in-reactor data. The in-reactor data come primarily from two Halden experimental rigs, instrumented fuel assembly (IFA)-504 and IFA-558

[†] The proposed revised standard has been completed by the ANS 5.4 subcommittee and submitted to the ANS 24 committee in January 2009 for submittal to ANSI for approval. Formal ANSI approval is expected by 2010.

(References 9 and 10), while a few data from IFA-633 were also used for verification of the revised ANS 5.4 release model coefficients. These three IFAs involved helium gas flowing through each of the fuel rods in the assembly to sweep out the radioactive isotopes such that the quantity of radioactive gas could be measured by detectors outside of the reactor taking into account decay during transport from the rods to the detector.

The details of how the in-reactor isotopic activities are measured and how they are converted to release data, R/B, for the radioactive isotopes of Kr-85m, Kr- 87, Kr-88 Kr-89, Kr-90, Xe-133, Xe-135, Xe-135m, Xe-137, Xe-138, Xe-139, I-131, I-133, and I-135 are provided in a Halden document (Reference 10) for the proposed revised standard. The release data (R/B) for the Kr-85m isotope were the principle release data used to verify the proposed revised ANS 5.4 model, which consisted of a total of 312 Kr-85m R/B data points from IFA-504, IFA-558, and IFA-633 (131, 175, and six data points, respectively). The Kr-85m release data were used because this isotope is relatively long-lived (4.48 hours) with a large activity peak that allowed it to be counted accurately with detectors, and a large quantity of these data existed. There were longer lived isotopes measured, such as Xe-133 (5.24 days) and Xe-135 (9.1 hours) but the measurement accuracies for these isotopes were significantly less than for Kr-85m. The proposed revised standard has also been compared and verified against I-131 R/B data from IFA-504 and IFA-558 but these data are of much lower quantity (only 17 R/B data points) due to difficulty in measuring this isotope. The I-131 release data are very important for verifying the proposed revised standard because it dominates most dose consequence analyses due to its large contribution of dose to the thyroid. The I-131 data also verify that the use of the Kr-85m data for establishing coefficients of the model and determining predictive uncertainties are reasonable. Further background information on the development of the standard based on the sweep gas data from Halden will be published in a background document sometime in the first or second quarter of 2009.

The range of the data in terms of rod average power and burnup is given in Figure 1. The rod power and burnup peaking factors for these rods are relatively low, between 1.06 to 1.09, compared to commercial fuel rod peaking factors of 1.1 to 1.3 for PWRs and 1.1 to 1.4 for BWRs.

2.1.1 Uncertainties in Revised ANS 5.4 Standard and Comparisons to Release Data

The predicted release fractions provided in this report, using the proposed revised ANS 5.4 standard, correspond to an upper bound of the Kr-85m data at a 95/95 upper tolerance level (UTL). This is achieved by multiplying the proposed revised ANS 5.4 best estimate predictions by a factor of 5 as recommended by this standard. The factor of 5 multiplier is derived assuming a non-normal distribution of the Kr-85m data. This factor of 5 multiplier on the best estimate predictions results in a conservative prediction of the I-131 release data as demonstrated in Figure 2 at a level greater than 95/95 tolerance level for these limited data. This is due to the fact that the multiplier is based on the prediction of the Kr-85m release data and not the I-131 release data. The factor of 5 is approximately a factor of 2 higher than what would be computed for the ANS 5.4 model predictions of the I-131 data. The extra conservatism was maintained for I-131, relative to that calculated for Kr-85m data, because some members of the standards sub-committee felt that the I-131 release measurements might be biased low by up to a factor of 2, therefore, a factor of 5 uncertainty is assumed for the I-131 predictions. The best estimate predictions of the I-131 data are provided in Figure 3 to demonstrate the accuracy of the model predictions.

2.1.2 Application of Proposed Revised ANS 5.4 Using a Fuel Performance Code

The application of the proposed ANS 5.4 standard for predicting the release of radioactive fission products requires the use of a fuel performance code that predicts fuel temperatures accurately up to the burnup and peak rod power levels achieved in current light-water reactor (LWR) cores (e.g., a peak pellet burnup of 70 GWd/MTU).

The ANS 5.4 standard also requires the use of a fuel performance code fission gas release model for the stable noble gases to predict the release of the long-lived isotopes of Kr-85, Cs-134, and Cs-137 and their associated uncertainties. This fuel performance code is required to accurately predict the release of the stable noble gases up to the burnup and peak rod power levels achieved in current LWR cores (e.g., a peak pellet burnup of 70 GWd/MTU). The 95/95 upper bound gap release prediction of these long-lived isotopes is based on the standard deviation of the stable noble fission gas fractions and the number of data points used to determine the standard deviation. The release data used to verify the code need to be based on fuel rods that operated near the peak power rods in an LWR core. The gap release fractions for Cs-134 and Cs-137 take into account the diffusion coefficient differences for the cesium isotopes relative to noble gases (see Section 3.1 below).

For this particular application, the FRAPCON-3.3 fuel performance code was selected. This code has been verified up to 70 GWd/MTU and beyond for both fuel centerline temperature and stable noble gas predictions. As noted in the proposed revised ANS 5.4 standard, other fuel performance codes may be used to estimate the fuel temperatures and gap release fractions for the long-lived isotopes of Kr-85, Cs-134, and Cs-137 if they have been verified against similar peak power rods up to peak pellet burnups of 70 GWd/MTU for LWR cores and have been approved by the NRC for licensing applications.

2.2 FRAPCON-3.3/ANS 5.4 Calculated Gap Release Fractions

The analyses using the proposed revised ANS 5.4 standard are divided into bounding PWR and BWR results, and sensitivity analyses have been performed to determine which of the current fuel designs are the most limiting in terms of release of fission products. The bounding PWR design was found to be a 14x14 fuel design and the bounding BWR design was a 9x9 fuel design. It should be noted that an 8x8 fuel design is slightly more bounding than the 9x9 design but U.S. reactors currently have very little or no 8x8 fuel in their cores, and the 8x8 design will not be used in future cores within the U.S.

Examination of the fuel temperature and fission gas release results from an earlier NRC report, NUREG-1754 (Reference 11), of analyses for different fuel designs also demonstrated that the 14x14 fuel design was most limiting of the PWR designs (14x14, 15x15, 16x16, and 17x17). This report also demonstrated that the 8x8 BWR fuel design was slightly more limiting in terms of temperatures and fission gas release than the 9x9 fuel design, and that the 10x10 design was the least limiting of BWR fuel designs.

2.2.1 PWR Analyses

The input parameters assumed for the 14x14 fuel design are provided in Table A-1 of Appendix A. The maximum power history assumed for this analysis is very important and is based on bounding the thermal-mechanical design linear heat generation rate (LHGR) limits in terms of peak nodal power (often referred to as the F_Q limit) for current cores licensed within the U.S. The power level in this analysis remains constant at the thermal-mechanical design limit up to a given burnup level, and then decreases with burnup. The decrease with burnup occurs because burnup depletes the U-235 to a level at which the remaining fissile material cannot sustain power operation at the peak F_Q limit at higher burnups for

current fuel core management schemes without other rods in the core exceeding this limit. Therefore, the assumed power history, given in Figure A-1 of Appendix A, is conservative at any given burnup level for current cores. It should be noted that running at the peak nodal power history in Figure A-1 for today's cycle lengths would exceed current burnup limits in the U.S.

In order for the power histories to be more realistic, but still bounding in terms of possible power operation, five different power histories were considered with each running at 90% of the peak node history in Figure A-1, with the exception of running at the LHGR limit for approximately 13 to 14 GWd/MTU burnup (peak pellet) for different burnup intervals as demonstrated in Figures A-2 to A-6 of Appendix A. The assumed PWR axial power shapes are given in Figure A-7. The upper bound PWR peak node histories are near the highest power Halden data in Figure 1 up to 56 GWd/MTU (rod average) burnup (or peak node burnup of ~ 60 GWd/MTU) with the data having a peak-to-average power of between 1.06 to 1.09. The data have a lower power rating than the PWR peak node history assumed in Figure A-1 above 60 GWd/MTU (peak node); therefore, there is a small extrapolation from 60 to 68 GWd/MTU (peak node) burnup. This small extrapolation is acceptable due to the large conservatism placed on the proposed revised ANS 5.4 release predictions, particularly the I-131 predictions that dominate the thyroid dose limits that are most limiting.

The calculated release fractions, R/B, for all of the radioactive isotopes of noble gases, iodines, and cesiums with half-lives greater than 1 hour for each of the five fuel rod power histories are provided in Table 1. The release rate, R, and birth rate, B, both have units of atoms/cm³-s with both including the decay of the specific isotope. Due to decay, an equilibrium R/B rate is established within 3 half-lives of an isotope (i.e., for iodine-131 with an 8-day half-life, equilibrium is achieved in 24 days, as long as the fuel temperature remains relatively constant during this time period). The isotope half-lives going from left to right in the table are decreasing starting with Kr-85 with a 10.76-year half-life with the exception of Cs-137 (a 30-year half-life) that is combined with Cs-134. All of the isotopes with half-lives greater than 1 year are conservatively treated as stable isotopes for ease of analysis as recommended by both the previous 1982 and proposed revised ANS 5.4 standard. The isotopes in Table 1 with half-lives greater than 1 day are those that dominate the radiological consequences due to external and internal dose, while generally the iodine release provides the smallest margins to dose limits due to their dose to the thyroid. Those isotopes with half-lives less than 1 day generally do not contribute much to dose due to their quick decay. It should be noted that the exceptionally high release for the I-132 isotope, even though it has a relatively short half-life of 2.28 hours, is due to the Te-132 precursor with a 3.2-day half-life and the fact that the proposed revised ANS 5.4 standard assumes that tellurium has a factor of 4 higher diffusion coefficient than the noble gases and iodine.

2.2.2 BWR Analyses

The input parameters assumed for the 9x9 fuel design are identified in Table A-1 of Appendix A. The maximum power history assumed for this analysis is very important and is based on bounding the LHGR technical specification limits for at the peak node for current BWR cores under normal operation licensed within the U.S. The peak node power level remains constant at the LHGR limit up to a given burnup level and then decreases with burnup. The decreasing power level beyond a given burnup level for BWRs is generally due to the need to meet rod internal gas pressure limits from the no cladding liftoff (NCLO) specified in Section 4.2 of the Standard Review Plan (Reference 12), as well as due to fissile depletion with burnup. Therefore, the assumed power history given in Figure A-1 of Appendix A is conservative at any given burnup level for current BWR cores. It should be noted that running at the power history in Figure A-8 for today's cycle lengths would exceed current burnup limits.

In order for the power histories to be more realistic, but still bounding in terms of possible power operation, six different power histories were considered with each running at 90% of the history in

Figure A-8 with the exception of running at the LHGR limit for approximately 13 to 14 GWd/MTU burnup (peak pellet) for different burnup intervals as demonstrated in Figures A-9 to A-13 in Appendix A. The assumed BWR axial power shapes are given in Figure A-14. The upper bound BWR peak node histories are near the highest power Halden data in Figure 1 up to 56 GWd/MTU (rod average) burnup (or peak node burnup of ~ 60 GWd/MTU) with the data having a peak-to-average power of between 1.06 to 1.09. Therefore, the data have a lower power peak rating than the BWR peak node history assumed in Figure A-8 above 60 GWd/MTU (peak node).

The BWR calculated release fractions, R/B, for the radioactive isotopes from each of the six fuel rod power histories are provided in Table 2. The caveats associated with Table 1 as discussed in Section 2.2.1 also apply here.

2.2.3 Assumed Analysis Uncertainties

The predicted release fractions calculated in this report are based on an upper bound tolerance of 95 percent probability with 95 percent confidence that the fractions are bounding. For the short-lived isotopes the 95/95 release fractions calculated with the proposed revised ANS 5.4 standard are determined by multiplying the best estimate predictions by a factor of 5 as recommended by the proposed revised standard. The FRAPCON-3.3 95/95 predicted release fractions are based on a standard deviation of 0.028 (absolute) from the prediction of the release of stable noble gases from 23 fuel rods (Reference 8) and assuming a normal distribution.

2.2.4 Discussion and Recommendations for Gap Release Fractions

Examining the release values in Tables 1 and 2 for PWR 14x14 and BWR 9x9 fuel designs demonstrates that the PWR design is the more limiting (i.e., has the higher release fractions). This is because the assumed PWR peak power histories are more aggressive at higher burnup levels. The BWR history starts off at a higher power level than the PWR history, 15 kW/ft versus 14 kW/ft, but begins to decrease at a lower burnup level such that at a peak node burnup of 34 GWd/MTU, the BWR peak power is 12.9 kW/ft while the PWR peak node is 14 kW/ft at the same burnup level. The BWR power history remains 1.1 to 1.35 kW/ft lower than the PWR history out to a peak node burnup of 66 GWd/MTU.

Further examination of Tables 1 and 2 demonstrates that the peak R/B release for the short-lived isotopes (less than 60-day half-life) always occurs at the highest burnup at which the highest rod power is achieved. This is because release increases with both increasing temperature and burnup, with temperature having the strongest impact. The peak release for all the short-lived isotopes is based on only the current temperature, production rate, and burnup. This is because the release of the short-lived isotopes reaches an equilibrium release quickly (within 3 half-lives) that is proportional to the current local fuel temperature, production rate (power), and burnup. Because the short-lived isotope release is more strongly dependent on fuel temperatures and power than burnup, the release decreases as power decreases such that the peak release in terms of number of curies occurs early in life. The decrease in R/B when power decreases is illustrated in Figure 4 where the predicted R/B for the I-131 isotope is plotted versus burnup for the PWR 14x14 Power History #3 shown in Figure A-4 in Appendix A. The increase in R/B with constant power as burnup increases is caused by an increase in fuel temperatures due to the degradation in fuel thermal conductivity with burnup. The increase of both temperature and burnup contributes to increased saturation of the grain boundaries resulting in a compounding increase in release with increasing burnup at constant power.

The peak release in terms of atoms or curies released, for the long-lived isotopes of Kr-85, Cs-134, and Cs-137 occurs at the end-of-life (EOL) or 62 GWd/MTU for the power histories assumed for this

analysis, even though the release fraction may decrease slightly with burnup. The release fraction, F , for long-lived isotopes is defined as the ratio of total atoms released to the gap to the atoms produced. This is different from the definition of the short-lived isotope release fraction, R/B , where R is the atom release rate in units of atoms/cm³-s and B is the atom production rate in units of atoms/cm³-sec. As noted, the release fraction, F , may decrease slightly before the EOL burnup is achieved but the isotope inventory is always increasing proportional to burnup, which increases at a greater rate than the decrease in release fraction. For example, the BWR Power History #4 has a peak Kr-85 release of 0.231 at a rod average burnup of 45.8 GWd/MTU while the release at 62 GWd/MTU (rod average) is 0.191. Therefore, the release at EOL results in 12 percent higher Kr-85 atoms released than at the lower burnup of 45.8 GWd/MTU, as calculated with the following relationship: $\{1-(0.191/0.231)*(62/45.8) = 0.12\}$. As noted above, the proposed revised ANS 5.4 standard conservatively does not account for decay of the long-lived isotopes; therefore, their inventory is always increasing proportional to burnup. This is illustrated in Figure 5, where the local release fraction is normalized to EOL burnup (proportional to stable isotope inventory) as a function of burnup using the following relationship.

$$F(\text{release at local burnup normalized to inventory}) = F(\text{at local burnup}) * (\text{local burnup}/\text{EOL burnup})$$

The latter term of (local burnup/EOL burnup) is proportional to the stable isotope inventory at the local burnup to the inventory at EOL. The release fraction in Figure 5 is predicted using the PWR 14x14 Power History #3 shown in Figure A-4 in Appendix A, the same as for the R/B I-131 prediction in Figure 4.

The recommended bounding releases for PWRs and BWRs are summarized in Table 3 based on the peak values in Tables 1 and 2 rounded up to two significant figures. The terminology in Table 3 is the same terminology as in Regulatory Guide 1.183, where “Other Noble Gases” represents all radioactive xenon and krypton isotopes (except Kr-85), “Other Halogens” represents those radioactive iodine isotopes with the exception of I-131 and I-132, and “Alkali Metals” represent the Cs-134 and Cs-137 isotopes. The gap release values in Table 3 are intended to replace the non-LOCA release fractions in Table 3 of Regulatory Guide 1.183 and the recommended gap release fractions in regulatory guides 1.5 and 1.25. The above methodology can be used to determine gap release fractions for a specific fuel design that may have less limiting power limits. The assumed fuel rod power history versus burnup is the major driving force for the calculated gap release fractions such that a fuel design with a lower power history than used in this analysis will have significantly lower release fractions.

3.0 Gap Release Fractions for Reactivity Initiated Accident

The total fission-product gap fraction available for release following any RIA should include the steady-state gap inventory (present from normal operation prior to the RIA event) plus any fission gas released during the RIA event. Conservative steady-state gap fractions from normal operation are provided in Table 3 of this report and the equations provided in this section will provide the conservative gap release fraction during the RIA event that need to be added to the steady-state gap release fractions from Table 3.

Regulatory Guides 1.183 and 1.77 recommend a gap release fraction of 0.10 for both noble gases and iodines. The stable noble gas release data from simulated RIA tests on PWR, BWR, and VVER test rods (shortened rod segments from actual commercially irradiated rods) are compiled in Appendix B from tests in CABRI (Reference 13), NSRR (References 14, 15, 16, and 17), and BGR (Reference 18) test reactors. These release data for stable isotopes are plotted in Figure 6 as a function of enthalpy increase. The release of stable noble gases in this figure applies to the long-lived Kr-85 isotope and demonstrates that above an enthalpy increase of ~ 40 cal/gm the upper bound Kr-85 release exceeds the 0.10 recommended release fraction for RIA in the regulatory guides. In addition, the release in Figure 6 is only the fraction of gas released during the RIA transient and does not include the release during normal operation. The release fractions provided in Figure 6 and Appendix B are relative to the total gas produced in the fuel. Therefore, a new recommended release will be provided in this report to replace the value of 0.10 specified in regulatory guides 1.77 and 1.183.

3.1 Discussion of RIA Release Data and Recommendations for Gap Fractions

From examination of the data in Appendix B, it is observed that the pulse widths from these different test reactors varied considerably with the CABRI tests having the widest pulse width between 9 to 76 millisecond (ms), the NSRR tests between 4 to 7 ms, and the BGR tests having a pulse width of 2 to 3 ms. Examination of the data in Figure 6 and the Appendix B table reveals that release increases with increasing enthalpy and that pulse width does not appear to have a large influence on FGR between ~ 2 to 76 ms. Also, fuel burnup may have an impact on release but the scatter in the data does not allow a definitive relationship to be established. The release fractions are from test rods with very short lengths such that the enthalpy increases and release values can be considered to be local rather than for a full-length LWR fuel rod.

An upper 95/95 tolerance level curve is presented in Figure 6 that bounds the RIA release data with the exception of three data points from NSRR tests of PWR segmented rods. The upper tolerance curve does not intercept the origin (a small positive release of 0.01 at zero enthalpy increase); consequently, a slightly different relationship than the 95/95 tolerance curve is recommended such that release fraction for long-lived isotopes can be bounded by the relationship:

$$F(\text{stable}) = 0.0022 * \Delta H$$

where ΔH is the enthalpy increase in cal/gm

This relationship provides a zero release at zero enthalpy increase.

The three short fuel test rods that are not bounded by the 95/95 curve are HBO-2, HBO-3, and HBO-4. These three test rods were refabricated from the same full-length PWR rod and then RIA tested in NSRR. The Japan Atomic Energy Research Institute (JAERI) papers and reports on these tests note that the release data from these three HBO specimens were anomalous compared to the rest of the release data from the NSRR tests. It should be noted that they are also anomalous to the remainder of the 32 other RIA FGR data in Figure 6. These JAERI reports noted that the fuel fabrication process for HBO-2, -3,

and -4 rods was different (labeled as Type-A fuel) than the rest of the HBO test series (labeled as Type-B fuel), but was similar to some of the fuel in the TK series test rods. For example, the TK-4 rod had Type-A fuel with similar burnup of 50 GWd/MTU but peak enthalpy was over twice as high for TK-4 as for HBO-2 (98 cal/gm versus 37 cal/gm, respectively), thus suggesting that TK-4 should have significantly higher FGR. However, the FGR in HBO-2 was over twice as high FGR as TK-4 (17.7 versus 8.3). This suggests that some unknown phenomenon caused higher FGR in HBO-2.

It has also been hypothesized that the higher FGR of the HBO-2, -3, and -4 rods may be due to their base irradiation (commercial reactor) powers being different from the other fuel rods in Figure 6 at equivalent burnup levels. However, examination of both TK-4 and HBO-2 test specimens demonstrated that they had similar base irradiation power histories. Therefore, base irradiation power histories do not explain the high release in the HBO-2, -3, and -4 rods unless there are errors in the base irradiation powers. Therefore, there is no clear explanation for why the HBO Type A fuel experienced significantly higher FGR than any other RIA tests performed in CABRI, NSRR (including other NSRR tests with Type-A fuel), and BGR at low fuel enthalpies.

Further examination of Figure 6 also shows that two NSRR BWR specimens and one CABRI PWR specimen provide significantly lower release than the majority of the other release data. The largest deviation was from a PWR CABRI test rod (REP Na-2) with the lowest burnup level (33 GWd/MTU) of the UO₂ test rods. The two NSRR BWR test rods (FK-1 and FK-3) were at relatively low burnups of 45 to 41 GWd/MTU, respectively. A qualitative theory of fission gas release can partially explain the lower release for these test rods based on the increase in interconnected fission gas bubbles on grain boundaries with increasing burnup. The fission gas release from the RIA test rods appears to be from the fracturing of the grain boundaries within the high burnup fuel rim and main body of the fuel and not due to diffusion during the RIA tests. These lower burnup fuel rods have little or no fuel rim and have less grain boundary gas in the main body of the fuel. Therefore, the lower burnup fuel will have less grain boundary gas than the higher burnup fuel with the latter having more inventory for release during the RIA. It is further noted that the low burnup (only 28 GWd/MTU) mixed oxide fuel (MOX) test rod from CABRI (REP Na-9) was within the release amounts of the higher burnup UO₂ test rods. This can be explained by the bubble interconnection process, which appears to occur in MOX (in the PuO₂ rich particles) at much lower burnups than for UO₂ (Reference 13).

In summary, a bounding (at a 95 percent probability with 95 percent confidence) relationship for Kr-85 release during a RIA has been developed that is only a function of peak fuel enthalpy increase. The bounding gap release fraction, F, for Kr-85 is defined as:

$$F(\text{Kr-85}) = 0.0022 * \Delta H$$

where ΔH is the enthalpy increase in cal/gm

There are no release data for the cesium, iodine, or short-lived noble gas isotopes from the RIA test rods. Therefore, their release fractions are estimated from the bounding relationship for stable noble gases and Kr-85 above. The release of the long-lived cesium isotopes (Cs-134 and Cs-137) can be estimated utilizing the ANS 5.4 standard recommendation in that cesium has a factor of 2 higher diffusion coefficient than the noble gases. Since release fraction is approximately proportional to the square root of the diffusion coefficient, the bounding release fraction for the long-lived cesium isotopes can be expressed as:

$$F(\text{Cs}) = 0.0022 * \Delta H * (2)^{0.5} = 0.0031 * \Delta H$$

where ΔH is the enthalpy increase in cal/gm

There are no release data for the short-lived isotopes for a RIA event, only release data for the stable noble gases exist; therefore, the short-lived isotope releases must be estimated from the stable noble gas release data. For short-lived isotopes, the time the gas is created (born) to the time it takes to be released

is critical for determining the release fraction, R/B, because the longer the holdup of gas in the fuel, the more R/B is reduced due to decay of the isotope.

The release of the short-lived isotopes of the noble gases and iodine during a RIA is similar to that for steady-state power operation once the grain boundary is saturated. This is because, once the grain boundaries are saturated during steady-state operation, there is no holdup of the gas on the grain boundaries and there is no holdup on grain boundaries during a RIA. The actual physical mechanism for release from the boundary is different between a RIA and that during steady-state operation. The RIA release is due to the fact that the large temperature increase within the fuel during this event fractures the grain boundaries, releasing the gas on the boundaries immediately. The steady-state release is caused by an interconnection of the (when bubble saturation is achieved) gas-filled bubbles on the boundary due to gas diffusion to the boundary opening the boundary for release. Both mechanisms release all of the grain boundary gas (radioactive and stable). The grain boundary saturation level for release decreases with fuel temperature for normal power operation such that an increase in fuel temperature over a few hours from a power ramp will also release grain boundary gas similar to a RIA event where the grain boundaries are fractured. Therefore, there is a ratio between the radioactive R/B release and the stable release fractions, F, that is primarily dependent on the fuel temperature increase (delta power increase) and burnup for both a RIA event and a slow power increase during normal operation. This ratio can then be used to estimate the release for a given isotope, such as I-131, which is of primary importance for dose calculations for a RIA.

Several calculations have been performed with the FRAPCON-3.3 code and the proposed revised ANS 5.4 model to examine the ratio between stable noble gas release and the release of I-131 for the BWR 9x9 and PWR 14x14 fuel design at power increases of 14, 26, 31, and 41 percent and at rod average burnups between 12 to 38 GWd/MTU. Only the release of the I-131 isotope was examined because it has the highest R/B release of the short-lived volatiles that has the largest impact on dose calculations. The ratio of the best estimate predicted release fractions between the stable noble gases and I-131 at a given time step when power is increased provides an indication of the delay time between when a I-131 atom is produced to when it is released during normal power operation with little holdup on the grain boundary. Examination of the calculational results demonstrates that the ratio between the stable isotopes and I-131 release (e.g., $F_{\text{stable}}/R/B_{\text{I-131}}$), is typically between 6 to 15 when the power is increased between 14 to 41 percent and rod average burnups are between 12 to 38 GWd/MTU. An increase in power of 41 percent for steady-state power operation results in a delta increase in stable release fraction of 0.15, which is the upper range of delta release of a RIA for an LWR. The ratio of $F_{\text{stable}}/R/B_{\text{I-131}}$ varies depending on power and burnup. This suggests that the release fraction from decay for I-131 is reduced by a factor of 6 to 15 due to the time for diffusion to the grain boundary and release. Therefore, it can be conservatively assumed that the diffusion from the fuel grain matrix to the grain boundary with no holdup on the grain boundary reduces the fractional release by a factor of 3 compared to the stable isotopes. As noted, the actual reduction in fractional release compared to the stable isotopes is most likely between a factor of 6 to 15, but without actual I-131 release data for test rods with simulated RIA power increases at various burnup levels, it is difficult to determine the exact factor of reduction in release.

The bounding gap release fraction, R/B, for I-131 and the other short-lived isotopes is defined as:

$$F(\text{short life isotopes}) = (0.33) * 0.0022 * \Delta H = 0.00073 * \Delta H$$

where ΔH is the enthalpy increase in cal/gm

The combined total RIA gap release fractions equals the steady-state gap fraction (Section 2) plus the transient releases provided in this section, as summarized in Table 4.

3.2 Example Determination of Gap Release Fractions for a RIA

Calculation of I-131 and Kr-85 combined gap fraction for an example fuel rod, which is calculated to experience cladding failure during a PWR control rod ejection event:

Due to the large variation in axial-dependent power peaking factors, the analyst chose to divide the fuel rod into three equal length axial regions. The peak radial average enthalpy change in each region is used to calculate the transient fission gas release component of the gap fraction within each axial region.

<u>Axial Region</u>	<u>Peak Enthalpy Increase</u>
Top (region #1)	150 cal/gm
Middle (region #2)	25 cal/gm
Bottom (region #3)	0 cal/gm
Combined $R/B_{(I-131)}$	$= 0.08 + ((0.00073*150/3)+(0.00073*25/3)+(0.00073*0/3))$ $= 0.123$
Combined $F_{(Kr-85)}$	$= 0.35 + ((0.0022*150/3)+(0.0022*25/3)+(0.0022*0/3))$ $= 0.478$

4.0 Conclusions and Limitations

The recommended bounding release fractions for accidents without large temperature increases are summarized in Table 3. The limitations of these release fractions are the power and burnup plots provided in Figure A-1 for PWRs and Figure A-8 for BWRs in Appendix A. If the peak rods in future cores exceed these power and burnup levels, the release values in Table 3 are no longer applicable.

The recommended bounding release fractions for RIA accidents are summarized in Table 4. These release fractions include both the steady-state gas inventory and the transient fission gas release.

5.0 References

1. Regulatory Guide 1.5, *Assumptions Used for Evaluating the Potential Radiological Consequences of a Steam Line Break Accident for Boiling Water Reactors*, March 1971.
2. Regulatory Guide 1.25, *Assumptions Used for Evaluating the Potential Radiological Consequences of a Fuel Handling Accident in the Fuel Handling and Storage Facility for Boiling and Pressurized Water Reactors*, March 1972.
3. Regulatory Guide 1.77, *Assumptions Used for Evaluating a Control Rod Ejection Accident for Pressurized Water Reactors*, May 1974.
4. Regulatory Guide 1.195, *Methods and Assumptions for Evaluating Radiological Consequences of Design Basis Accidents at Light-Water Nuclear Power Reactors*, May, 2003.
5. Regulatory Guide 1.183, *Alternative Radiological Source Terms for Evaluating Design Basis Accidents at Nuclear Power Reactors*, U.S. Nuclear Regulatory Commission, 2000.
6. Lanning, D.D., C.E. Beyer, and K.J. Geelhood. 2005. *FRAPCON-3 Updates, Including Mixed Oxide Properties*, NUREG/CR-6534 (PNNL-11513) Vol. 4., U.S. Nuclear Regulatory Commission, Washington D.C.
7. American National Standard Institute, ANSI/ANS 5.4, *Method for Calculating the Fractional Release of Volatile Fission Products from Oxide Fuel*, American Nuclear Society, November, 10, 1982.
8. Lanning, D.D., C.E. Beyer, and C.L. Painter. 1997. *FRAPCON-3: Modifications to Fuel Rod Material Properties and Performance Models for High-Burnup Application*, NUREG/CR-6534 (PNNL-11513) Vol. 1., U.S. Nuclear Regulatory Commission, Washington D.C.
9. Turnbull, J.A., *The Treatment of Radioactive Fission Gas Release Measurements and Provision of Data for Development and Validation of the ANS 5.4 Model*, HWR-667, Halden Project report, February 2001 (available in the NRC Public Document Room).
10. White, R.J. and J.A. Turnbull, *The Measurement of Fission Product Release Using the Gas Flow Rigs: A Review of Experiments, Methodology and Results from 1980-1997*, HWR-553, Halden Project report, February 1998.
11. O'Donnell, G.M., H.H. Scott and R.O. Meyer, *A New Comparative Analysis of LWR Fuel Designs*, NUREG-1754, December 2001.
12. Standard Review Plan, Section 4.2, NUREG-0800 Revision 3, U.S. Nuclear Regulatory Commission, March 2007.
13. Lemoine, F., J. Papin, J. Frizonnet, B. Cazalis, and H. Rigat, "The Role of Grain Boundary Fission Gases in High Burn-Up Fuel Under Reactivity Initiated Accident Conditions," *Fission Gas Behavior in Water Reactor Fuels - Seminar Proceedings Cadarache France*, 26-29 September 2000.
14. Fuketa, T., H. Sasajima, Y. Tsuchiuchi, Y. Mori, T. Nakamura, and K. Ishijima, "NSRR/RIA Experiments with High Burnup PWR Fuels," *Proceedings of 1997 International Topical Meeting on Light Water Fuel Performance*, Portland, Oregon, March 2-6, 1997.
15. Fuketa, T., T. Sugiyama, H. Sasajima and F. Nagase, "NSRR RIA-simulating Experiments on High Burnup LWR Fuels," *Proceedings of the 2005 Water Reactor Fuel Performance Meeting*, Kyoto, Japan, pp. 633-645, October 2-6, 2005.
16. Nakamura, T., M. Yoshinaga, M. Takahashi, K. Okonogi, and K. Ishijima, "Boiling Water Reactor Fuel Behavior Under Reactivity-Initiated-Accident Conditions at Burnup of 41 to 45 GWd/tonne U," *Nuclear Technology*, Vol. 129, pp 141-151, February 2000.

17. Nakamura, T., K. Kusagaya, T. Fuketa and H. Uetsuka, "High-Burnup BWR Fuel Behavior Under Simulated Reactivity-Initiated Accident Conditions," *Nuclear Technology*, Vol. 138, pp 246-259, June 2002.
18. Yegorova, L. et al, *Experimental Study of Narrow Pulse Effects on the Behavior of High Burnup Fuel Rods with Zr-1%Nb Cladding and UO₂ Fuel (VVER Type) under Reactivity-Initiated Accident Conditions: Program Approach and Analysis of Results*, NUREG/IA-0213, Vol. 1, May 2006.

Table 1. PWR Fuel Rod Release Fractions, R/B, for Isotopes with Half-Lives Greater Than 1 Hour for Five Bounding Power Histories up to 68 GWd/MTU Peak Node Burnup and Rod Average 62 GWd/MTU (All Burnups are in GWd/MTU)

Power History	Kr-85 ¹ Best Estimate	Kr-85 ¹ @95/95	Cs-134 ¹ & 137 @95/95	I-131 ² @95/95 (burnup)	Xe-133 ² @95/95	I-133 ² @95/95	Xe-135 ² @95/95	I-135 ² @95/95	Kr-85m ² @95/95	Kr-88 ² @95/95	I-132 ² @95/95	Kr-87 ² @95/95
#1	0.228	0.294	0.358	0.030 (31)	0.027	0.017	0.013	0.013	0.012	0.009	0.091	0.006
#2	0.232	0.298	0.394	0.050 (22)	0.045	0.029	0.022	0.022	0.022	0.015	0.15	0.011
#3	0.243	0.309	0.410	0.073 (32)	0.066	0.042	0.032	0.032	0.031	0.022	0.22	0.016
#4	0.261	0.327	0.434	0.052 (37)	0.046	0.030	0.022	0.022	0.022	0.015	0.158	0.011
#5	0.277	0.348	0.457	0.041 (33)	0.037	0.023	0.018	0.018	0.017	0.012	0.12	0.009

¹ Release at EOL

² Maximum at burnup in parenthesis

Table 2. BWR Fuel Rod Release Fractions, R/B, for Isotopes with Half-Lives Greater Than 1 Hour for Five Bounding Power Histories up to 70 GWd/MTU Peak Node Burnup and Rod Average 62 GWd/MTU (Burnups are rod average in GWd/MTU)

Power History	Kr-85 ¹ Best Estimate	Kr-85 ¹ @95/95	Cs-134 ¹ & 137 @95/95	I-131 ² @95/95 (burnup)	Xe-133 ² @95/95	I-133 ² @95/95	Xe-135 ² @95/95	I-135 ² @95/95	Kr-85m ² @95/95	Kr-88 ² @95/95	I-132 ² @95/95	Kr-87 ² @95/95
#1	0.147	0.213	0.273	0.026 (12)	0.023	0.015	0.011	0.011	0.010	0.008	0.080	0.006
#2	0.153	0.219	0.282	0.036 (20)	0.033	0.021	0.016	0.016	0.015	0.011	0.111	0.008
#3	0.163	0.229	0.296	0.032 (27)	0.029	0.018	0.014	0.014	0.013	0.009	0.097	0.007
#4	0.191	0.257	0.336	0.029 (39)	0.026	0.016	0.012	0.012	0.012	0.009	0.088	0.006
#5	0.179	0.245	0.319	0.019 (20)	0.017	0.011	0.008	0.008	0.008	0.006	0.058	0.004

¹ Release at EOL

² Maximum at burnup in parenthesis

Table 3. PWR and BWR Fuel Rod Peak Gap Release Fractions, R/B, Based on Peak Values from Tables 1 and 2³

Isotope	Gap Release Fractions - 95/95 UTL			Current RG 1.183 Table 3
	Calculated PWR 14x14 design	Calculated BWR 9x9 design	Maximum	
Kr-85	0.348	0.257	0.35	0.10
I-131	0.073	0.036	0.08	0.08
I-132	0.225	0.111	0.23	0.05
Other Nobles	0.031	0.016	0.04	0.05
Other Halogens	0.042	0.021	0.05	0.05
Alkali Metals	0.457	0.336	0.46	0.12

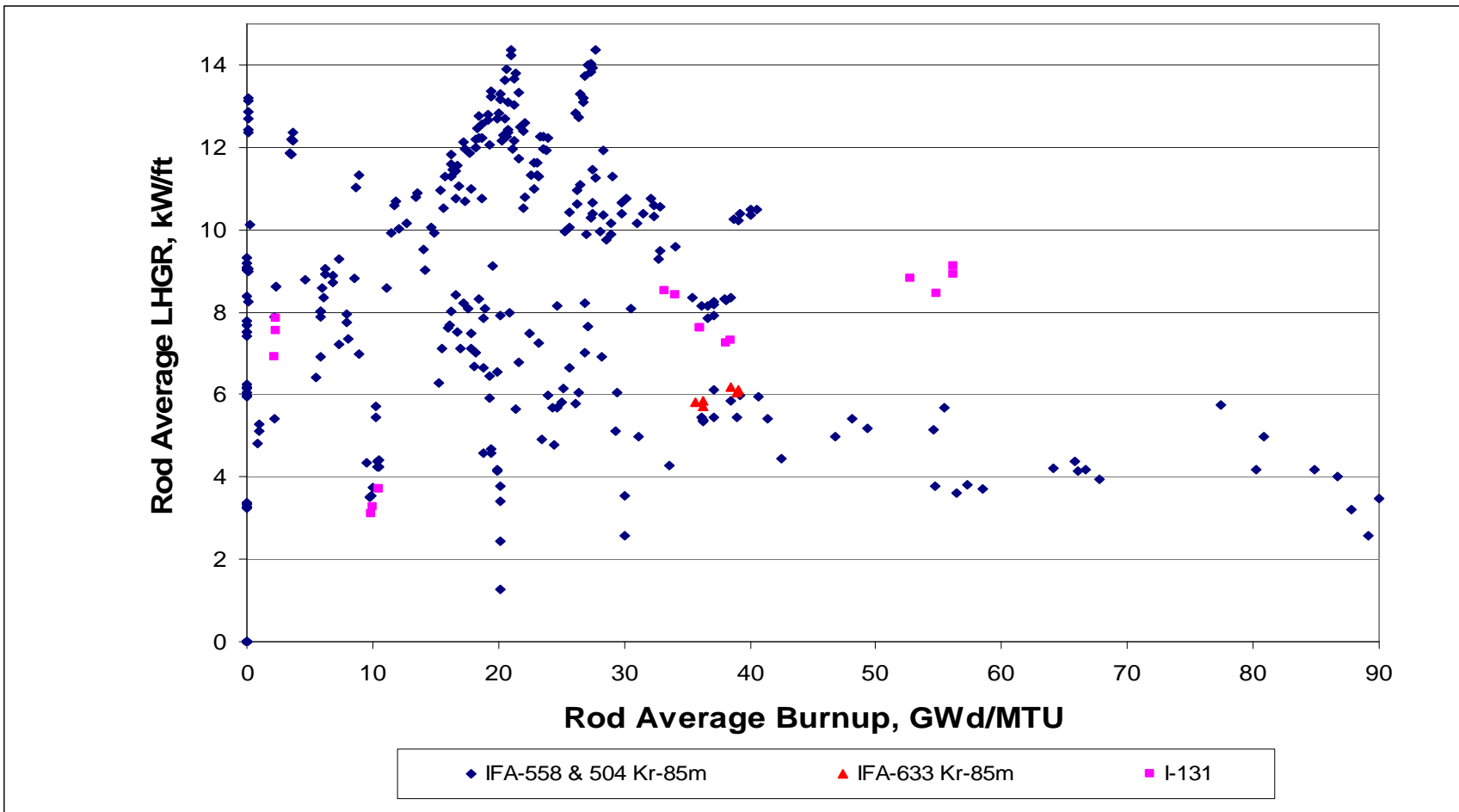
³ Gap fractions for non-LOCA events with exception of RIA events

Table 4. Local Gap Release Fractions for Reactivity Initiated Accidents

Isotope	Combined RIA Release Fraction ^{4,5}
Kr-85	((0.35) + (0.0022 * ΔH))
I-131	((0.08) + (0.00073 * ΔH))
I-132	((0.23) + (0.00073 * ΔH))
Other Nobles	((0.04) + (0.00073 * ΔH))
Other Halogens	((0.05) + (0.00073 * ΔH))
Alkali Metals	((0.46) + (0.0031 * ΔH))

⁴ ΔH= increased fuel enthalpy during RIA event, cal/gm

⁵ Assumes no fuel melting



**Figure 1. Operating Range of Data Used to Develop and Verify the ANS 5.4 Model
Data from Instrumented Sweep Gas Experiments in the Halden Reactor**

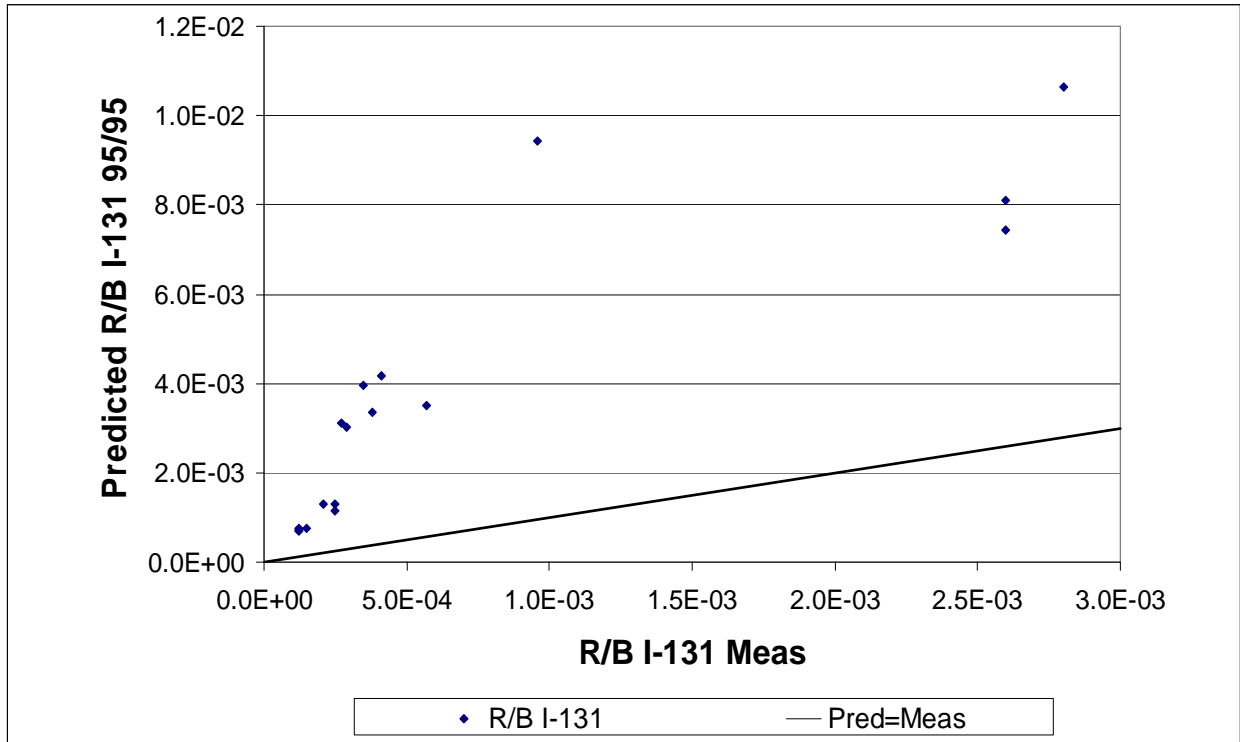


Figure 2. Revised ANS 5.4 Standard Model Comparison of Prediction to Measured I-131 Release Data Assuming a Factor of 5 Multiplier on Prediction Results in a 95/95 UTL

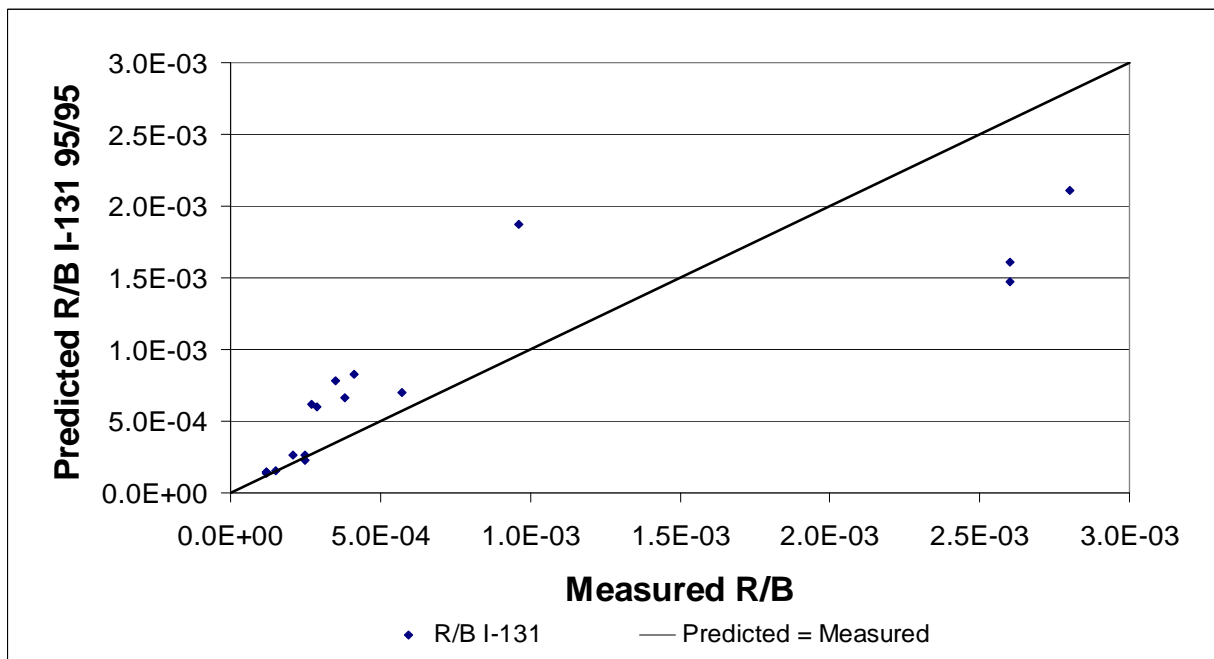


Figure 3. ANS 5.4 Model Best Estimate Prediction of R/B I-131 Data from Halden Experiments IFA-504 and IFA-558

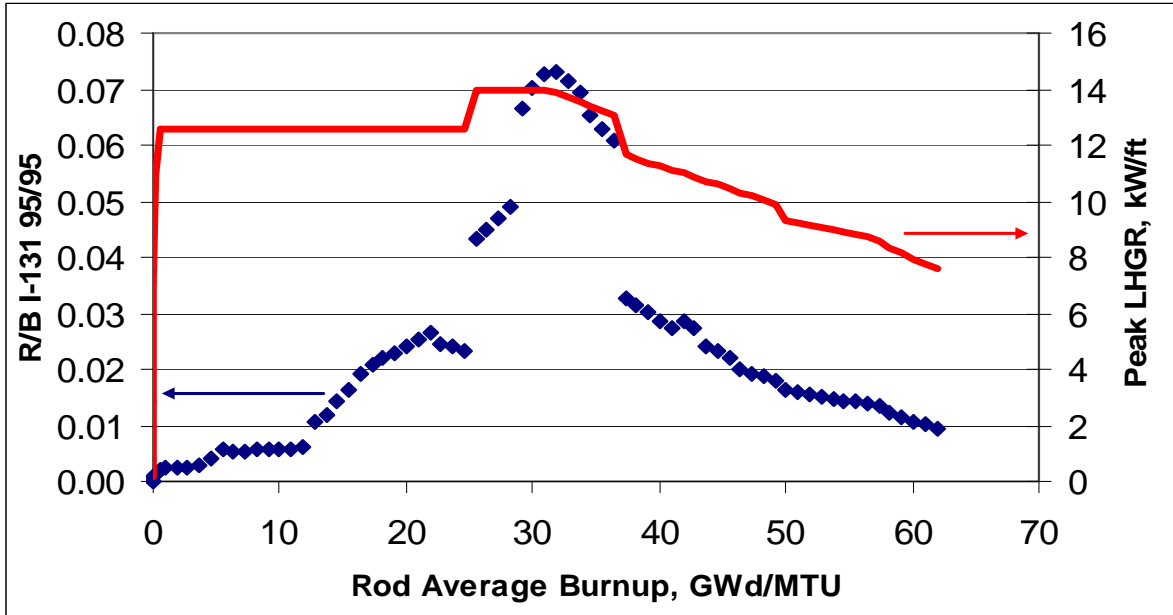


Figure 4. Predicted R/B Release for I-131 as a Function of Burnup Illustrating Peak Release Occurs at the Maximum Burnup at which Maximum Rod Power is Achieved

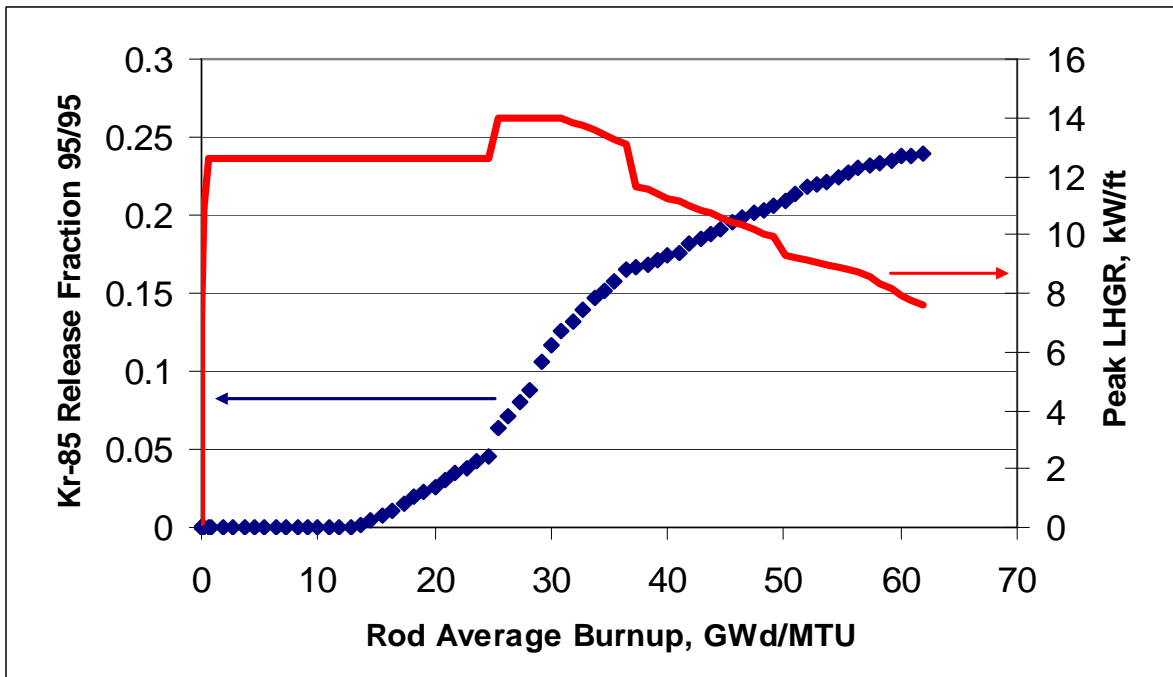


Figure 5. Predicted Release Fraction Normalized to Produced Inventory for Kr-85 (Long-Lived) Isotope as a Function of Burnup Illustrating Peak Release Occurs at EOL

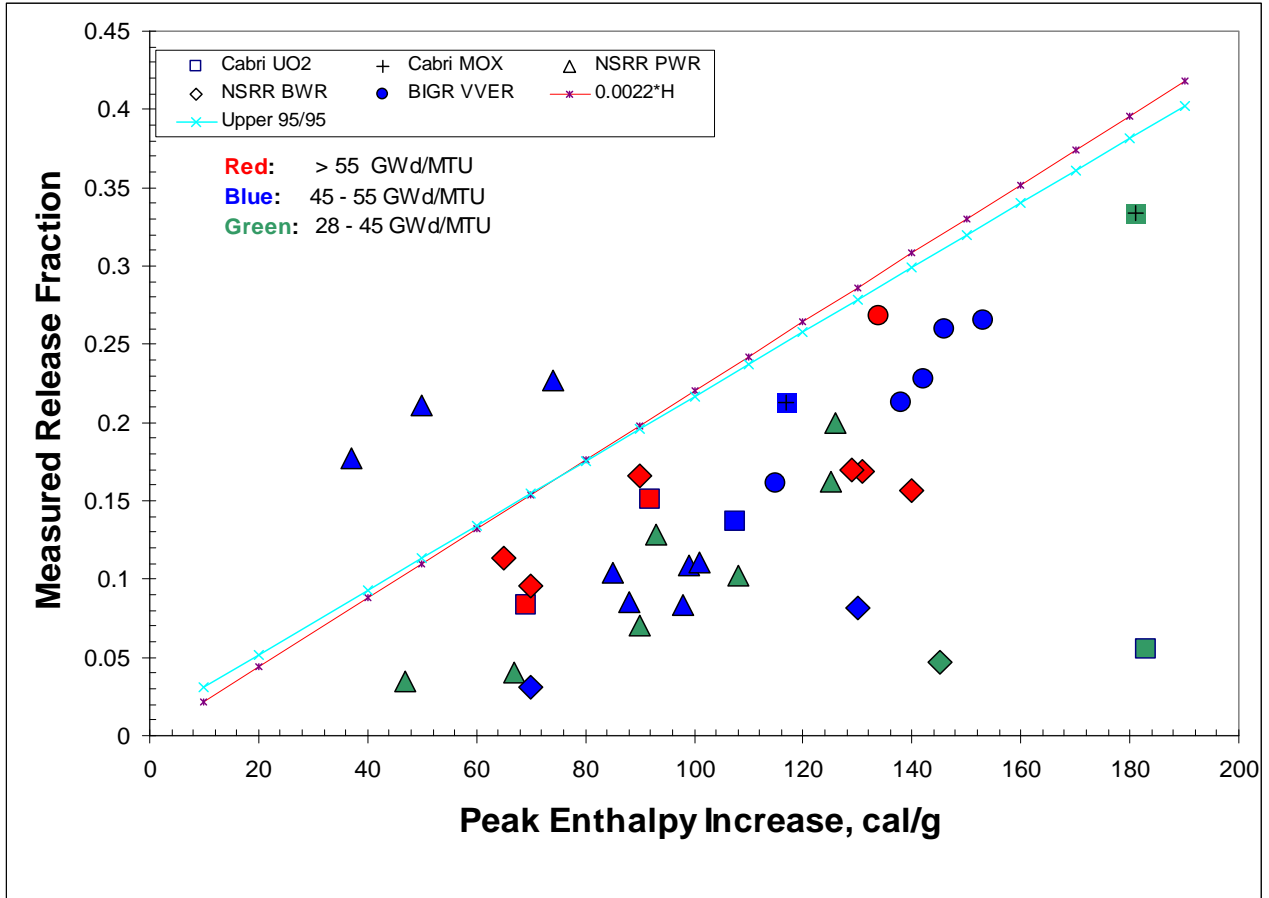


Figure 6. Stable Fission Gas Release Data as a Function of Peak Fuel Enthalpy Increase from Simulated RIA Tests in CABRI, NSRR, and BGR Test Reactors

Appendix A: Code Input including Power Histories and Axial Power Shapes Used for FRAPCON-3.3/ANS 5.4 Analyses

Table A-1. FRAPCON-3.3 Input Parameters for PWR and BWR Analyses

Description of Design Parameter	PWR 14x14	BWR 9x9
Pitch (mm, <i>in</i>)	14.7, 0.58	13.0, 0.510
Cladding OD (mm, <i>in</i>)	11.2, 0.44	10.8, 0.424
Cladding Thickness (mm, <i>in</i>)	0.737, 0.029	0.711, 0.028
Cladding ID (mm, <i>in</i>)	9.70, 0.382	9.35, 0.355
Diametral Gap Thickness (mm, <i>in</i>)	0.191, 0.0075	0.203, 0.008
Fuel Pellet Diameter (mm, <i>in</i>)	9.51, 0.374	9.14, 0.360
Plenum Spring Diameter (mm, <i>in</i>)	9.51, 0.374	9.14., 0.360
Pellet Length (mm, <i>in</i>)	12.7, 0.5	11.2, 0.44
Dish Diameter (mm, <i>in</i>)	4.57, 0.18	5.81, 0.2288
Dish Depth (mm, <i>in</i>)	0.305, 0.012	0.216, 0.0085
Plenum Length (mm, <i>in</i>)	254, 10	245, 9.64
Turns in Plenum Spring	30	29
Plenum Spring Wire Diameter (mm, <i>in</i>)	1.32, 0.052	1.4, 0.055
Helium Fill Gas Pressure (MPa, <i>psi</i>)	2.07, 300	1.03, 150
Active Fuel Length (m, <i>in</i>)	3.66, 144	3.81, 150
System Coolant Pressure (MPa, <i>psi</i>)	15.5, 2250	7.27, 1055
Coolant Inlet Temperature (°C, °F)	288, 550	277, 530
Coolant Flow Rate ($\times 10^3$ kg/s-m ² , $\times 10^6$ lb/hr-ft ²)	3.60, 2.65	1.67, 1.23
Enrichment (atom %)	4.95	5
Pellet Density (% TD)	96	96
Limit on Pellet Density Increase (% TD)	0.7	0.7
Fuel Surface Roughness (μ m, <i>in</i>)	1.6, 6.3×10^{-5}	1.5, 5.9×10^{-5}
Cladding Surface Roughness (μ m, <i>in</i>)	1.0, 3.9×10^{-5}	0.9, 3.6×10^{-5}
Cladding Material	ZIRLO	Zircaloy-2
Cold Work (%)	50	0

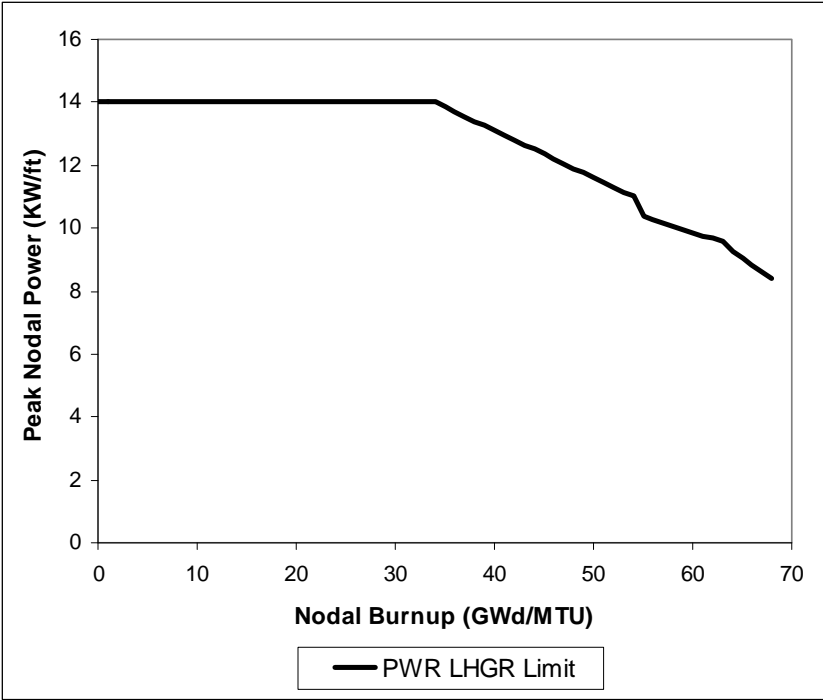


Figure A-1. LHGR Bounding Limit for PWRs Up to 34 GWd/MTU (Peak Nodal Burnup), Beyond this Burnup LHGR Based on Depletion for Current Cores

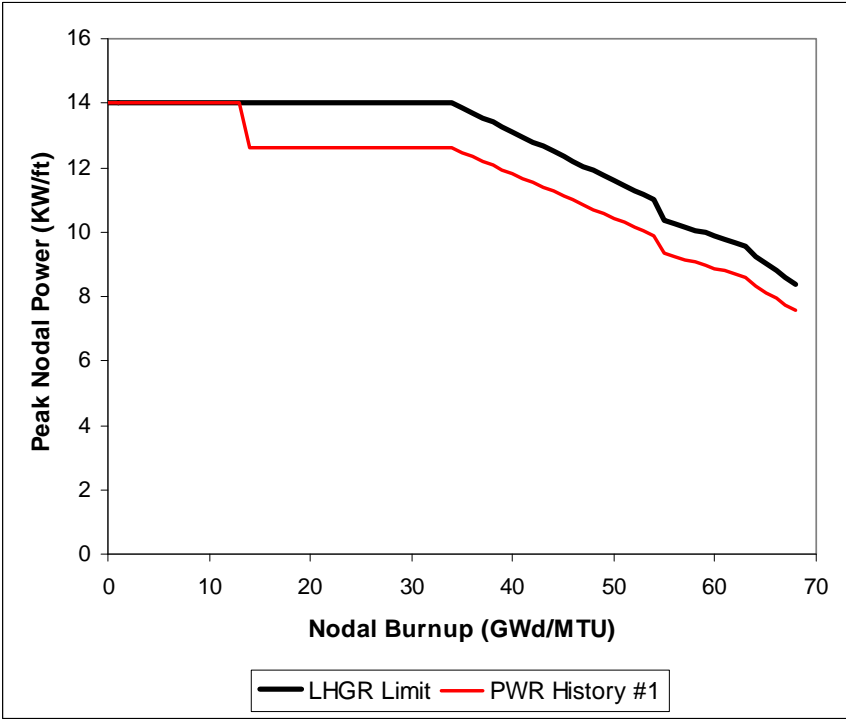


Figure A-2. Assumed PWR Power History #1

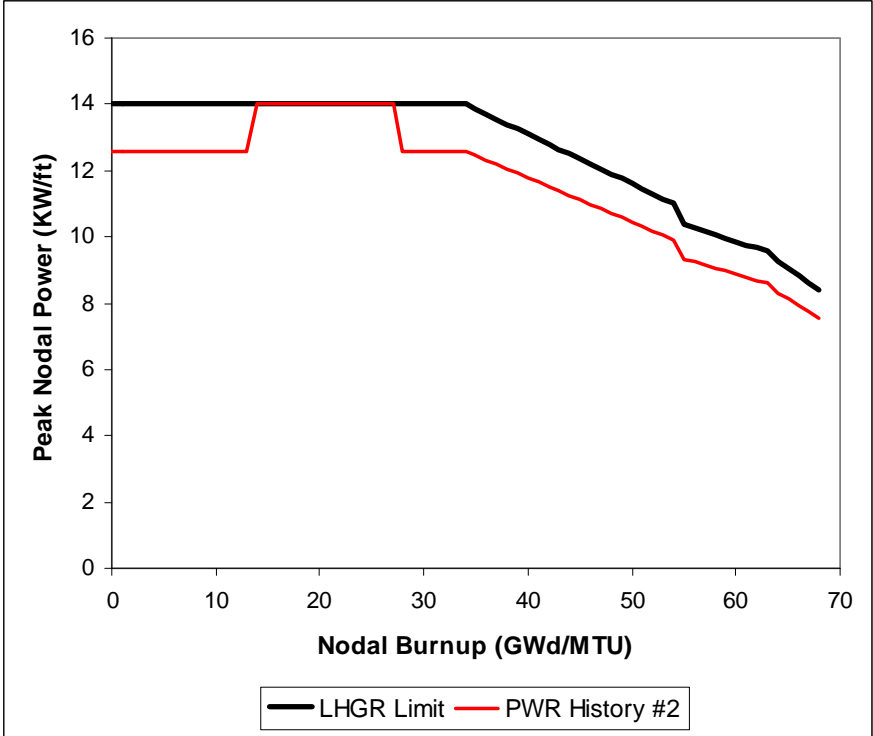


Figure A-3. Assumed PWR Power History #2

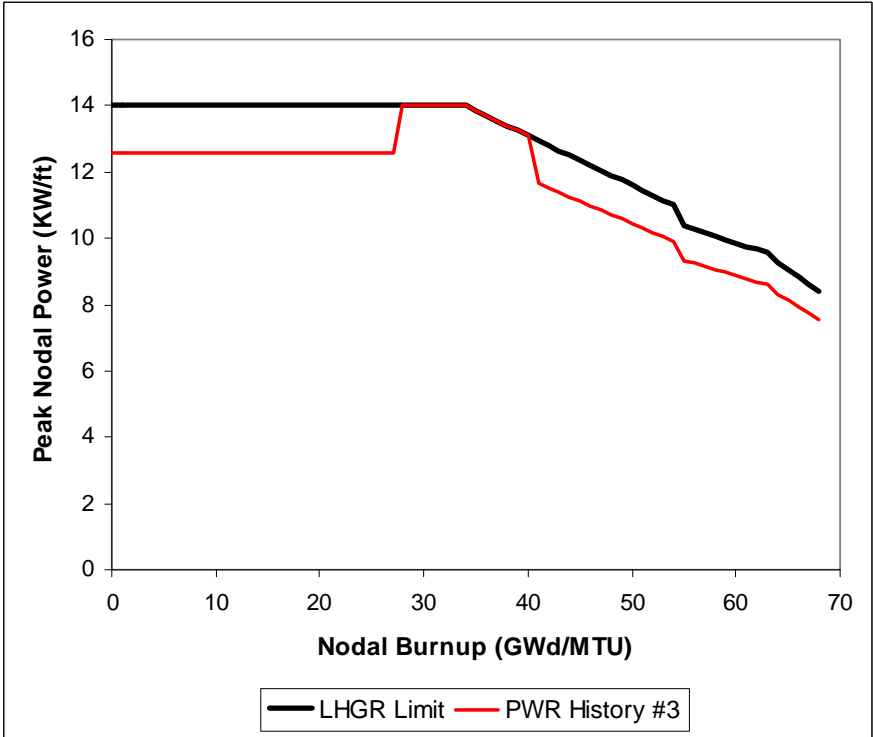


Figure A-4. Assumed PWR Power History #3

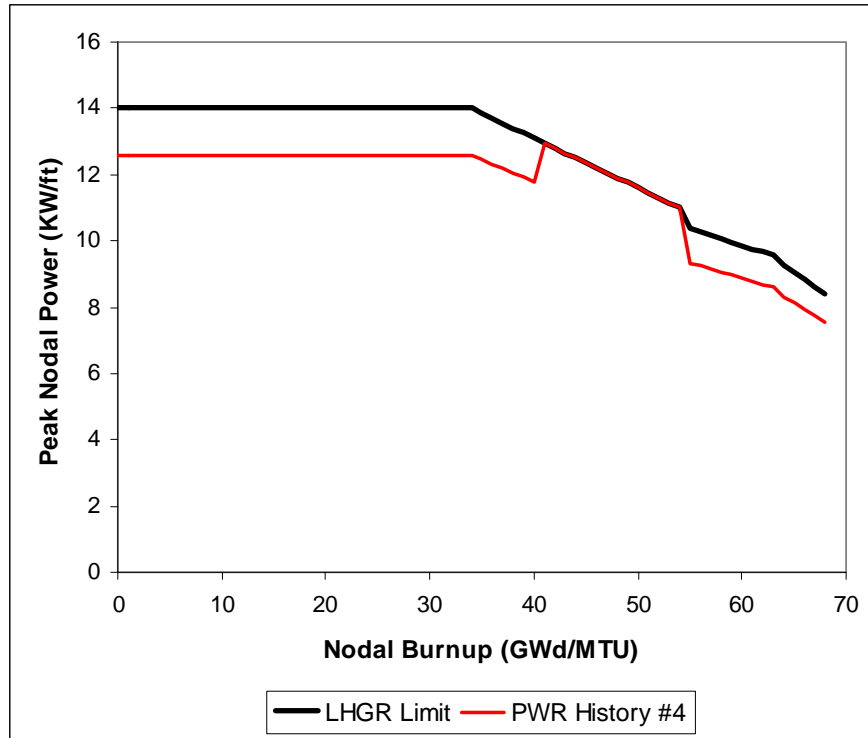


Figure A-5. Assumed PWR Power History #4

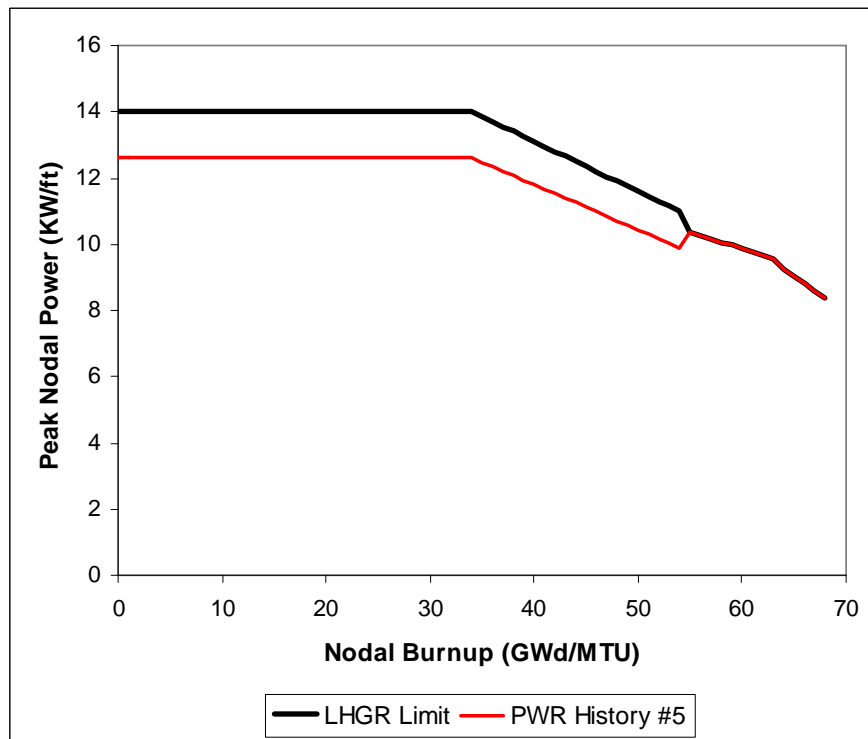


Figure A-6. Assumed PWR Power History #5

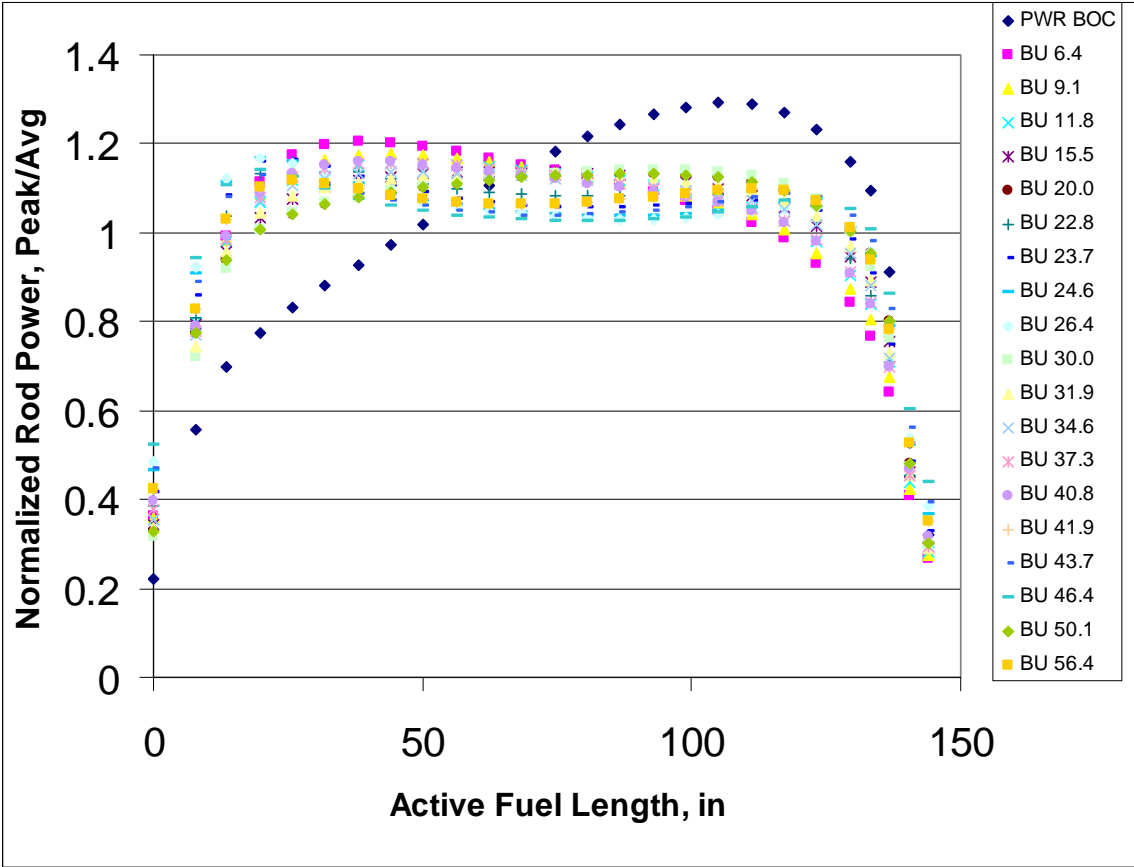


Figure A-7. PWR Normalized Axial Power Shapes, the BU Label is the Rod Average Burnup (GWd/MTU) Level the Shape Begins

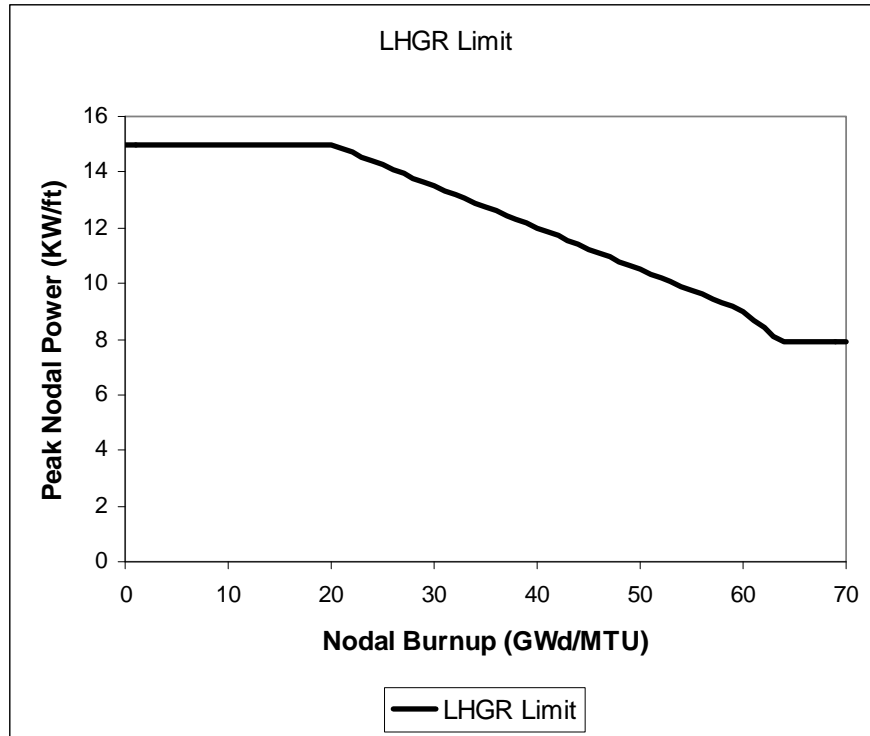


Figure A-8. LHGR Bounding Limit for BWRs Up to 70 GWd/MTU (Peak Nodal Burnup)

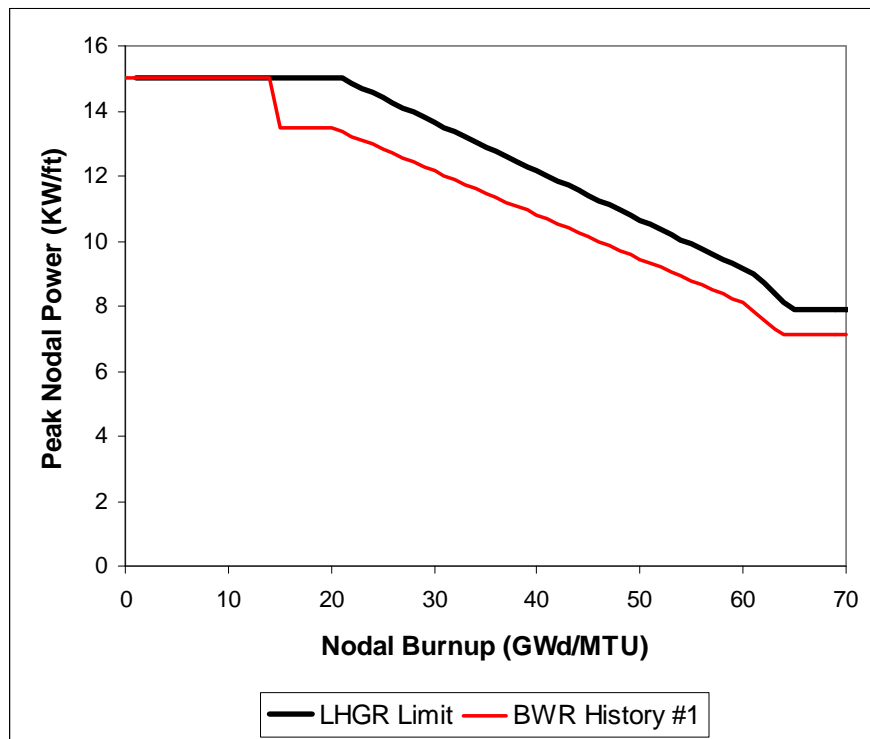


Figure A-9. Assumed BWR Power History #1

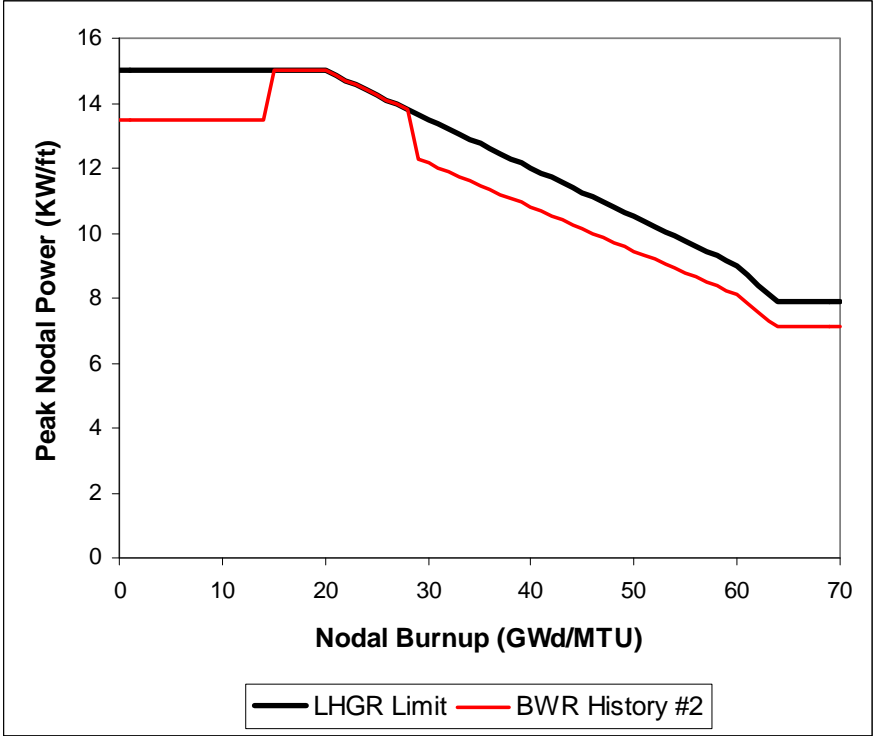


Figure A-10. Assumed BWR Power History #2

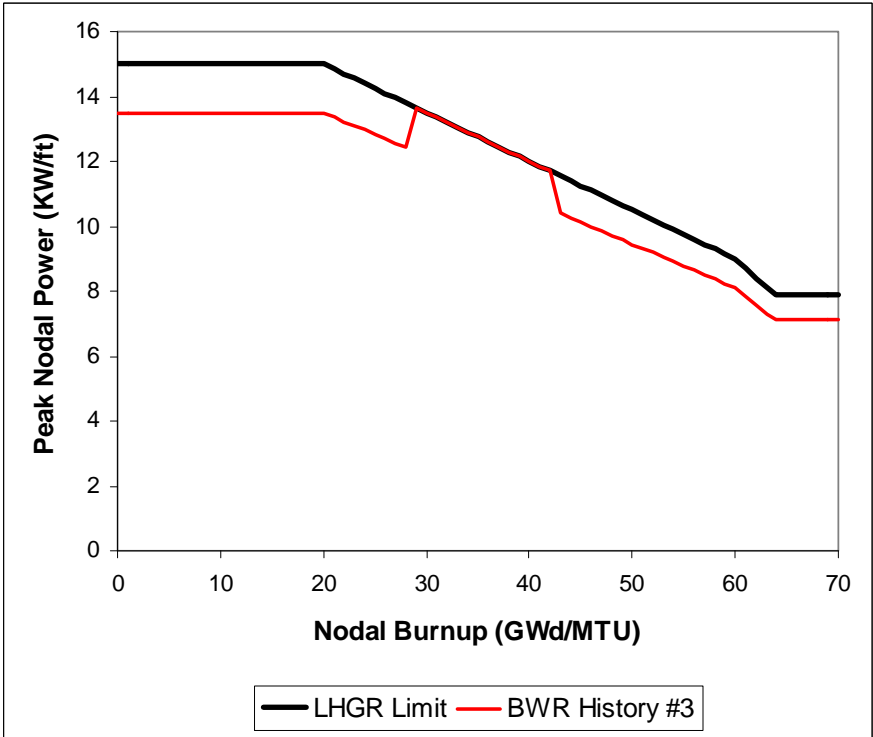


Figure A-11. Assumed BWR Power History #3

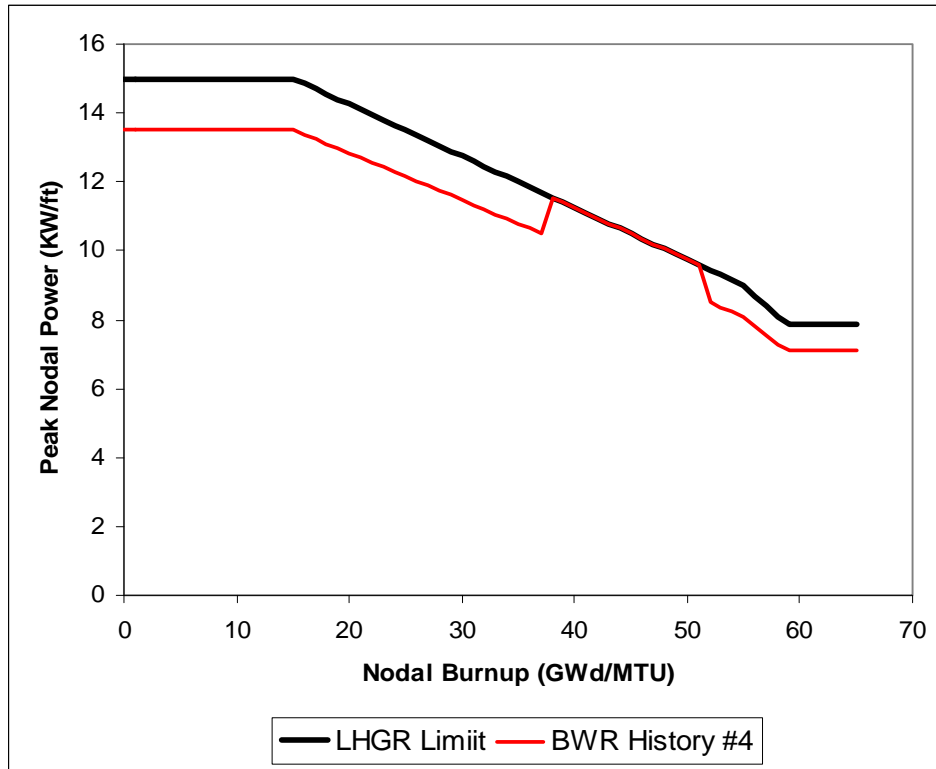


Figure A-12. Assumed BWR Power History #4

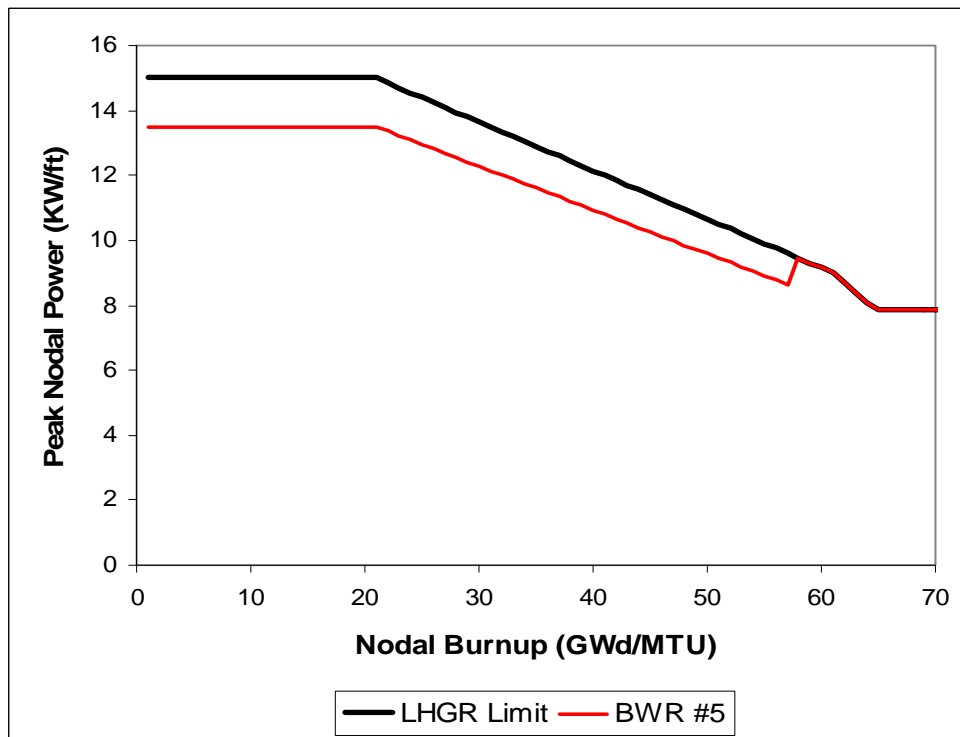


Figure A-13. Assumed BWR Power History #5

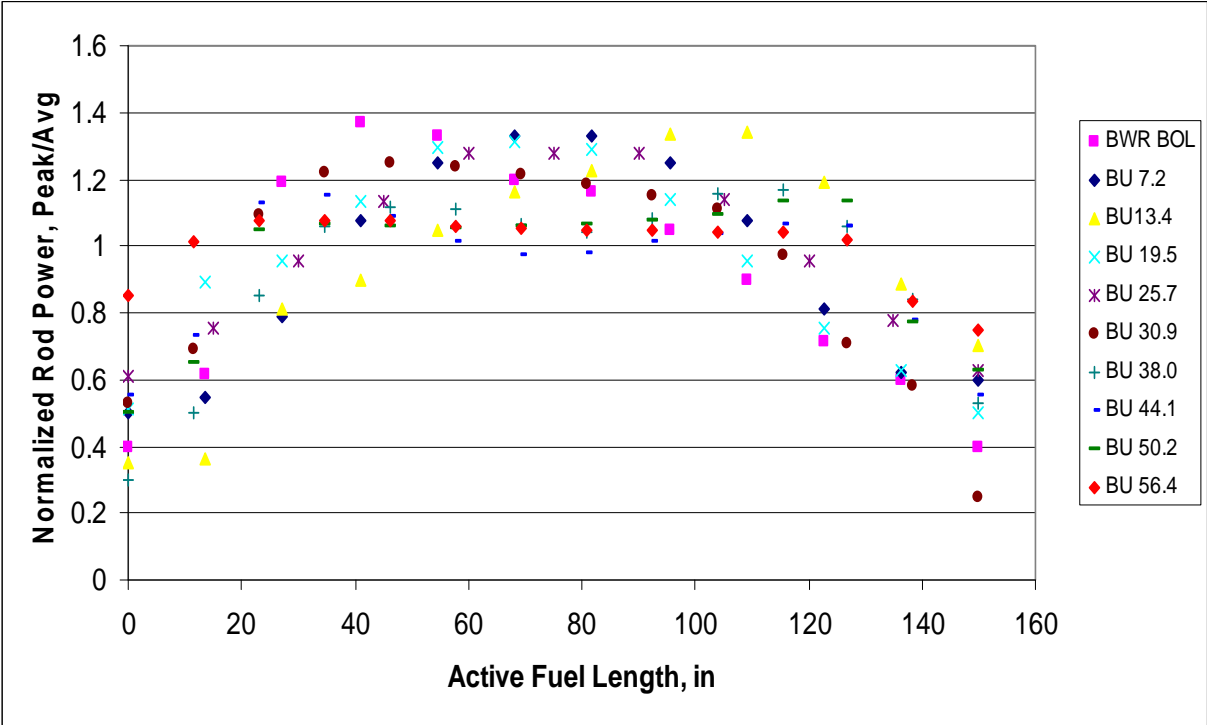


Figure A-14. BWR Normalized Axial Power Shapes, the BU Label is the Rod Average Burnup (GWd/MTU) Level at Which the Axial Shape Begins

Appendix B: Compilation of Fission Gas Release Data from RIA Tests in CABRI, NSRR and BGR

Test Rods	Burnup, GWd/MTU	Enthalpy Deposited, cal/gm	Pulse width, ms	Enthalpy Increase ΔH , cal/gm	FGR Fraction
CABRI PWR					
Na2	33	207	9.6	183	0.0554
Na3	53.8	122.2	9.5	107.5	0.137
Na4	62	95	76.4	69	0.083
Na5	64	104	8.8	92	0.151
Na6	47	156	32	117	0.213
Na9	28.1	233	33	181	0.334
NSRR PWR					
TK1	38	126	4.8	126	0.2
TK3	50	99	4.8	99	0.109
TK4	50	98	4.8	98	0.083
TK5	48	101	4.8	101	0.111
TK6	38	125	4.8	125	0.162
HBO2	50.4	37	4.8	37	0.177
HBO3	50.4	74	4.8	74	0.227
HBO4	50.4	50	4.8	50	0.211
HBO6	49	85	4.8	85	0.104
HBO7	49	88	4.8	88	0.085
OI-2	39.2	108	4.4	108	0.102
MH1	38.9	47	4.5	47	0.035
MH3	38.9	67	4.5	67	0.04
GK1	42.1	93	4.6	93	0.128
GK2	42.1	90	4.6	90	0.07
NSRR BWR					
FK-1	45.4	130	4.5	130	0.082
FK-2	45.4	70	7	70	0.031
FK-3	41	145	4.5	145	0.047
FK-4	56	140	4.3	140	0.157
FK-5	56	70	7.3	70	0.096
FK-6	61	131	4.3	131	0.169
FK-7	61	129	4.3	129	0.17
FK-8	61	65	7.3	65	0.113
FK-9	61	90	5.7	90	0.166
BIGR VVER					
RT2	47-49	115	2	115	0.161
RT3	47-49	138	2	138	0.213
RT1	47-49	142	2	142	0.228
RT5	47-49	146	2	146	0.26
RT6	47-49	153	2	153	0.265
RT7	60	134	2	134	0.268



Pacific Northwest
NATIONAL LABORATORY

902 Battelle Boulevard
P.O. Box 999
Richland, WA 99352
1-888-375-PNNL (7665)

www.pnl.gov



U.S. DEPARTMENT OF
ENERGY